The 1976 Oppenheimer lectures: Critical problems in plasma astrophysics. II. Singular layers and reconnection*

Roald Z. Sagdeev

Space Research Institute, Moscow, U.S.S.R.

The J. Robert Oppenheimer Lectures are given annually at the Institute for Advanced Study, Princeton, New Jersey, by a distinguished visiting scientist who has made outstanding research contributions in a field of current interest and who is recognized for his ability to communicate progress in his area of expertise to a broad spectrum of physical scientists. The lecturer summarizes the progress and significance of work in his field in a series of two talks. The lectures are named in honor of J. Robert Oppenheimer, former Professor in the School of Natural Sciences, Institute for Advanced Study, and the third Director of the Institute. This paper presents the text of the second lecture on the topic of singular layers and reconnection.

CONTENTS

I. INTRODUCTION

In this lecture, I should like to discuss some important laboratory and astrophysical phenomena concerned with the development of discontinuities in plasma systems. In general, many different types of discontinuities are possible. Clearly, those which persist for long times are most important. For this reason, we shall deal here with only two kinds of discontinuities: shocks and neutral layers. These are also the ones of greatest practical importance. Let us begin with shocks.

II. SHOCKS

The present status of the collisionless shock problem can be summarized as follows (Sagdeev, 1966; Biskamp, 1973). Collisionless shocks have been proved to exist both in laboratory and in space plasmas. Their physics is qualitatively understood, and comprehensive quantitative models have been developed for a variety of soluble limiting cases. Other cases can and have been treated with numerical simulation.

That collisionless shocks should even exist, however, was not obvious in the early days of investigation. Let us therefore develop the concept of a collisionless shock by first reviewing the collisional shock of conventional gas dynamics. This shock arises as a result of nonlinear wave steepening, which may conveniently be discussed in terms of the Riemann solution (Fig. 1).

We consider the temporal evolution of a finite-amplitude perturbation $\tilde{v}$ at t_0. If P and ρ are the unperturbed pressure and mass density, respectively, then each point $(\tilde{v}, P, \rho)$ on the initial profile will propagate with a velocity

$$\left(\frac{dx}{dt}\right)_v = \left(\frac{dP}{d\rho}\right)^{1/2} + \tilde{v} . \tag{1}$$

As we see from Fig. 1, this gives rise to a steepening of the profile. When this steepening becomes sufficiently large, dissipative processes begin to compete. Eventually, the balance between dissipation and the $\mathbf{v} \cdot \nabla \mathbf{v}$ steepening leads to a shock structure, whose thickness we can estimate from

$$v \cdot \nabla v \sim \nu (\partial^2 v / \partial x^2) .$$

Here ν is the kinematic viscosity, of order $l v_t$, where l is the mean free path, and v_t is the molecular thermal speed. Thus the shock thickness Δ_{sh} becomes

$$\Delta_{sh} \sim \frac{\nu}{\tilde{v}} \sim \frac{1}{(\mathfrak{M} - 1)} l ,$$

where $\mathfrak{M}$ is the Mach number [we used $\tilde{v} \sim (\mathfrak{M} - 1) c_s$].

If one attempts to apply these arguments directly to the conditions of space plasma, say the solar wind, one fails rather badly. Since the Coulomb mean free path is measured in astronomical units, whereas the observed shock-like behavior occurs over much shorter
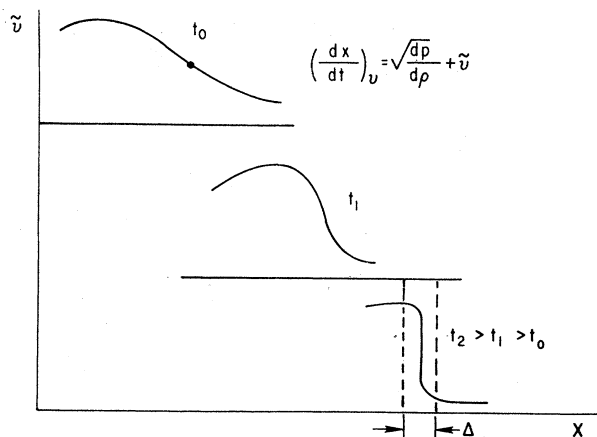

FIG. 1. The steepening process and formation of a conventional collisional shock. Definition of the shock thickness Δ.
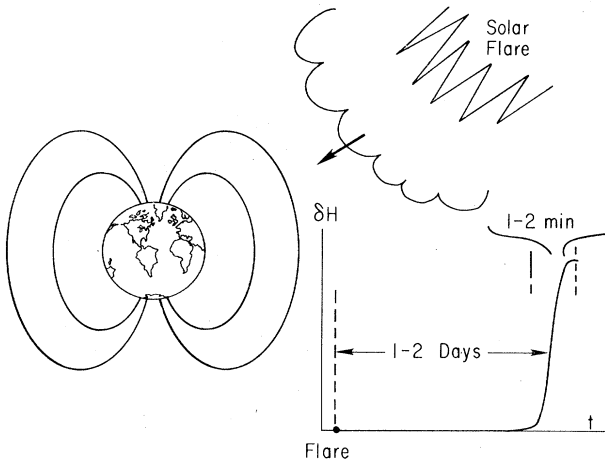
FIG. 2. The sudden onset of magnetic storms caused by plasma from solar flares impinging on the earth.

distances, it seems absurd to use the collisonal shock concept. Also, in the rarified laboratory plasmas we have the case $l \gtrsim L$, where L is the size of the device, but again almost discontinuous behavior is observed over scales short compared to L. Clearly, a new concept is called for.

Since the earliest days of investigation of the plasma state, it has been recognized that the collective behavior of even the collisionless plasma can be of crucial importance. Among the many hypotheses related to anomalous collective effects was the concept of a collisionless shock. The first clear observational evidence for this idea came from the study of phenomena related to solar flares. In particular, an apparent paradox arose when one considered the sudden onset of magnetic storms caused by the solar flares (Fig. 2). It was natural to argue that the geomagnetic field should be strongly disturbed when the plasma cloud ejected by the flare arrived in the vicinity of the earth. If Δv represents the characteristic velocity spread of the cloud ions, then one would expect the characteristic rise time Δt for the magnetic storm to be of order $\Delta t/t \sim \Delta v/v$. The actual measured rise time is extremely short, with Δt of the order of several minutes; this would imply an unbelievably small velocity spread: $\Delta v/v \sim 10^{-3}$. One could hardly imagine that any natural process of plasma acceleration, especially of an explosive type, could produce such monoenergetic ions. However, in 1955, T. Gold suggested that there would be, in fact, no paradox if the interplanetary medium could propagate shocks. Further support for the collisionless shock concept came from basic plasma theory and rapid development of the guiding center models for magnetized plasma. Finally, in the early 1960's, a fairly self-consistent picture of collisionless shocks began to emerge from theoretical analysis. This was confirmed in some detail by laboratory experiments, measurements of the solar wind, and numerical simulations.

Two distinct limiting cases bound the scope of the collisionless shock problem. These are:

1) fluid-like behavior (which can occur even for col-

lisionless plasma) and

2) nonfluid behavior (particle free-streaming).

The first case is simpler (though far from simple!). It is based on the observation that, under certain conditions, the collisionless plasma can exhibit many of the features of fluid-like media. One could readily expect such behavior, for example, for the cross-field motion of particles frozen to magnetic field lines. If one considers motion on scales much larger than a gyroradius, then the $E \times B$ drift adequately represents the particle behavior (if we ignore free-streaming along the lines). This guiding center description has equations of a structure identical to those of magneto-gas dynamics. The only difference is that for the plasma we need a specific heat ratio of $\gamma = 2$, to take proper account of the adiabaticity of the magnetic moment $\mu \equiv mv_\perp^2/B = \mathrm{const}$.

For strongly nonisothermal plasmas $(T_e \gg T_i)$, the fluid-like behavior persists even in the absence of a magnetic field. This we can see from the following arguments. Suppose that the electric potential changes sufficiently slowly so that the electrons adjust to a Boltzmann distribution

$$n_e = n_0 \exp(e\phi/T_e).$$

Assume also that ion thermal motion is negligible. We can then use a truncated form of the moment equations for the ions,

$$\partial n_i/\partial t + \nabla \cdot (n_i v_i) = 0, \tag{1a}$$

$$M[\partial v_i/\partial t + (v_i \cdot \nabla)v_i] = -e\nabla \phi, \tag{1b}$$

together with

$$\nabla^2 \phi = -4\pi e(n_i - n_e), \tag{1c}$$

$$n_e = n_0 \exp(e\phi/T_e). \tag{1d}$$

For scales much larger than the Debye length, we can to lowest order replace Poisson's equation by the quasineutrality condition $n_i = n_e = n$. For $e\phi/T_e < 1$, we can also approximate $\exp(e\phi/T_e) \simeq 1 + e\phi/T_e$. The resulting model

$$\frac{\partial n}{\partial t} + \nabla \cdot (nv) = 0,$$

$$M\left[\frac{\partial v}{\partial t} + (v \cdot \nabla)v\right] = -T_e \nabla(n/n_0),$$

corresponds to a fluid picture with $\gamma = 1$. [The eigenmodes in this case—ion acoustic waves or phonons—would exhibit only a small additional amount of kinetic damping $\sim(m/M)^{1/2}$ due to the electron Landau resonance.] Naturally, all such fluid-like models will exhibit the Riemann behavior (Fig. 1). Arguing as before, we arrive at a need of some process to balance the nonlinear steepening. This turns out here to be a dispersion effect, arising from the deviation from quasineutrality, which competes for sufficiently small scales. Let us examine this effect qualitatively. A typical form of dispersion relation would be

$$\omega/k = (\mathrm{const})[1 \pm k^2 \delta^2 + O(k^4)],$$

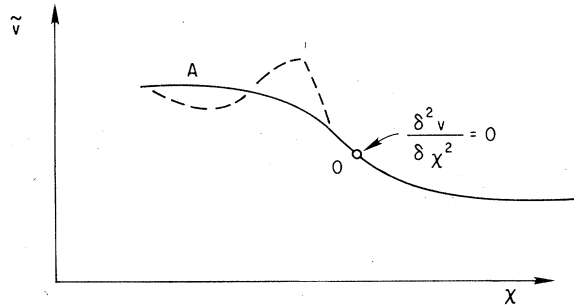where δ is a constant depending on physical parameters.

FIG. 3. Initial (——) and final (- - -) profiles when dispersion $[\Delta(\omega/k) = -k^2\delta^2]$ is effective in balancing $v \cdot \nabla v$ steepening.

The $k^2\delta^2$ term corresponds to the dispersive effect of higher-order derivatives in the equation of motion. We can qualitatively assess their effect by inserting a new term in the Riemann solution: $\Delta(\omega/k) = \pm k^2\delta^2 = \mp \delta^2 \partial^2/\partial x^2$. Now, consider the initial profile of Fig. 3 and examine the subsequent behavior in the vicinity of $\partial^2 v/\partial x^2 = 0$. Let us first consider the choice of lower sign in the expression for $\Delta(\omega/k)$. Then, to the right of the point where $v'' = 0$, we will have $\Delta(\omega/k) < 0$, which is just what we need to compensate the $v \cdot \nabla v$ steepening. On the other hand, since $\Delta(\omega/k) < 0$ just to the left of point 0, points near Sec. A, where $\partial^2 v/\partial x^2$ again $\to 0$, will attempt to overtake those just to their right and the profile will develop the shape shown in the dotted lines. We can expect this competition of effects to result in a steady state, where all quantities vary as x-ut, with u being the shock speed. For the model (1) with $T_e \gg T_i$, the appropriate calculations are simplest. We do not now impose quasineutrality. Reduction of (1) then leads to a second-order differential equation for the potential (Sagdeev, 1966)

$$\frac{d^2\phi}{dx^2} = -\frac{d}{d\phi} V(\phi) , \qquad (2a)$$

where

$$V(\phi) = 4\pi n_0 e\left[-\left(\frac{M}{e}\right) u \left(u^2 - \frac{2e\phi}{M}\right)^{1/2} - \left(\frac{T}{e}\right)\exp\left(\frac{e\phi}{T}\right)\right] + C , \qquad (2b)$$

and C is an integration constant.

It is convenient to visualize the solution of this equation by thinking of the analogous problem of a particle moving in a nonlinear potential well V [in (2), we replace
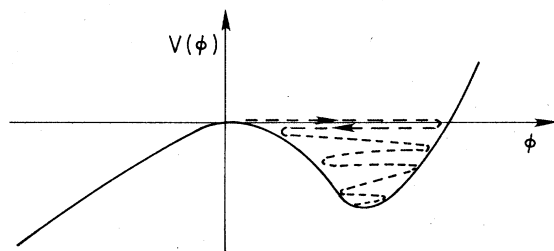

FIG. 4. The potential $V(\phi)$ for an ion acoustic shock with soliton boundary conditions $[C = 4\pi n_0 (Mu^2 + T)]$. Dashed line is soliton solution (no dissipation); dotted line is behavior with small amount of dissipation (see Fig. 5).
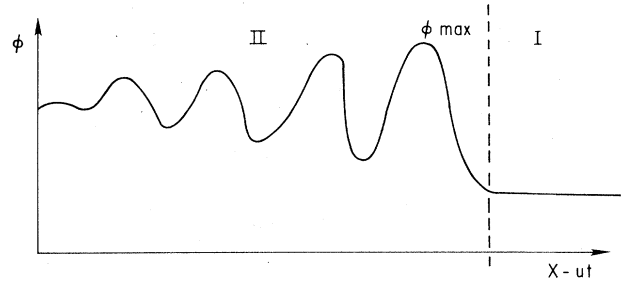

FIG. 5. The oscillatory shock, or train of solitons, which results when a small amount of dissipation is added to a soliton solution (see also Fig. 4). I: Preshock (unperturbed region; II: postshock (perturbed) region.

$x \to t, \phi \to x]$ (Fig. 4). The solution with $\phi \to 0$ as $x \to \infty$ represents a solitary wave (soliton). Even a very small (even symbolic) amount of dissipation would produce an entire wave train of solitons (particle falling slowly into the bottom of the well). Figure 5 illustrates such a structure and shows that we can introduce the concept of an oscillatory shock which connects the unperturbed (preshock) plasma (I) with the perturbed (postshock) plasma (II). In this case, one should modify the Hugoniot–Rankine relations to include the energy and momentum of the oscillatory structure (train of solitons).

If we solve Eq. (2) with the soliton conditions $\phi' \to 0$ as $\phi \to 0$, we can find the dependence of u (or $\mathfrak{M} \equiv u/c_s$) on the maximum potential ϕ_{max}:

$$u^2 = \left(\frac{T}{2M}\right) \left[\exp\left(\frac{e\phi_{max}}{T}\right) - 1\right]^2 \Big/ \left[\exp\left(\frac{e\phi_{max}}{T}\right) - 1 - \frac{e\phi_{max}}{T}\right] .$$

A critical amplitude, above which propagation is impossible, is given by $e\phi_{max} = 1/2Mu^2$, the point at which ions can no longer get across the potential barrier. Thus there are no solutions if $\mathfrak{M} > \mathfrak{M}_c \simeq 1.6$, or $\phi > \phi_{max} \simeq 1.3$ T_e/e.

One assumption, in particular, of the above treatment needs to be discussed carefully. To what extent can we trust the Boltzmann approximation $n \sim \exp(e\phi/T_e)$ for collisionless electrons? If one starts with Maxwellian electrons $\exp(-mv^2/2T)$ going "up the hill" $-e\phi$, there seems to be no problem: $f(v) \sim \exp[-(1/2 mv^2 - e\phi)/T]$; the shape of the distribution does not change. However, consider the opposite case of electrons rushing "downhill" into the potential well (an example would be the electric potential of a soliton). Here, if one follows the development of the well in time (Fig. 6), one concludes
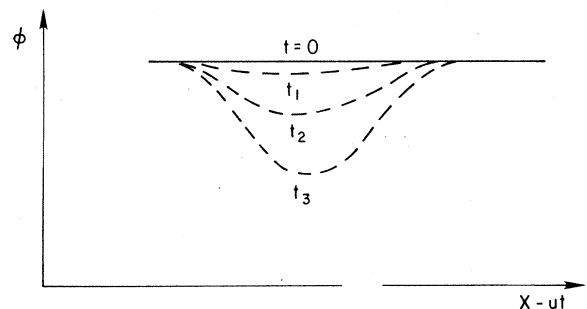

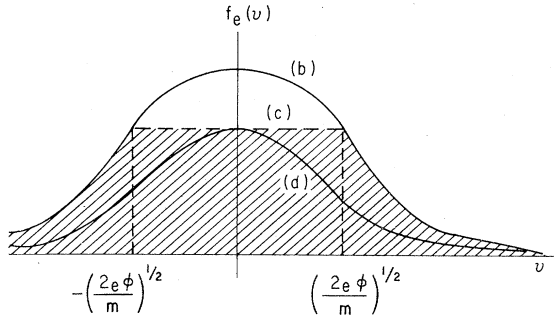FIG. 6. Schematic development of potential well with time.

FIG. 7. (a) Maxwellian at $\phi = 0$. (b) Maxwell–Boltzman distribution [$\sim \exp(e\phi/T)$]. (c) [shaded area] distribution with trapping included.

that the electrons trapped in such a well will have a distribution significantly different from Maxwellian. Indeed, while the well is growing, each time electrons approach the well from either side, a small fraction of them will be trapped if they enter with sufficiently small velocities. Those which were already trapped sink yet deeper, conserving their adiabatic invariants as they do so. Such an argument implies that the velocity distribution for trapped electrons is constant, equal to the value just outside the well:

$$f_{\text{trapped}} = f(v = 0).$$

In Fig. 7 the shaded area represents the electron density $n_e(\phi)$ modified to include the effects of trapping. This agrees with the Boltzmann distribution only for $e\phi/T \ll 1$; otherwise, $n_e(\phi) < n_0 \exp(e\phi/T)$. This modification has some quantitative effects for the solitons. For $T_i = 0$, the critical Mach number becomes $M_c \simeq 3.1$ instead of 1.6, for example. However, we should not take either of these values too literally for many reasons, of which we mention only two. Even the initial electron distribution could be non-Maxwellian in the most general case. Furthermore, the critical Mach number is very sensitive to even a very small ion thermal spread; we do not have good quantitative control of this feature.

For any case where the plasma behaves in a fluid-like fashion, the steady-state oscillatory structure of the shock is easy to find. One has just to solve a system of ordinary, nonlinear differential equations similar to Eq. (1). Generally, the characteristic space scale for these steady-state waves is of the order of the char-
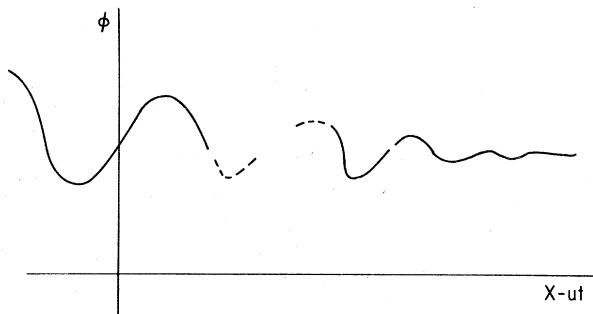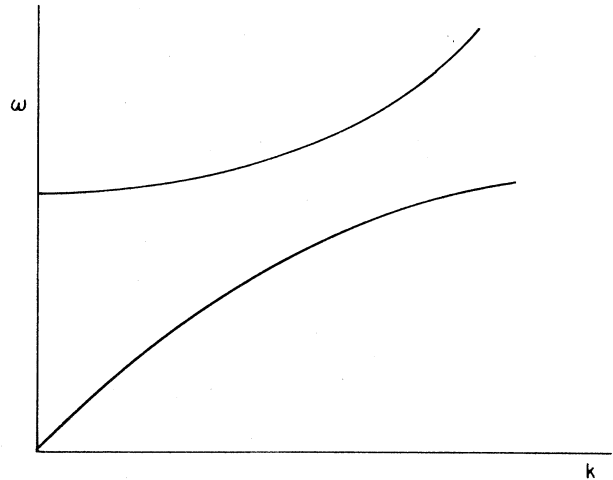

FIG. 9. A typical dispersion law with two branches.

acteristic dispersion length δ. For example, a collision-less shock perpendicular to a strong magnetic field ($8\pi nT/B_0^2 \ll 1$) would appear as a wave train of solitons with $\delta \sim c/\omega_p$. The amplitude of the magnetic field would not exceed $3B_0$, and the Mach number would be less than two (Sagdeev, 1966).

If we considered the other possible case $\Delta(\omega/k) = k^2 \delta^2$, we would obtain rarefaction solitons instead of compressional ones. This is the case when the shock propagates at angles slightly oblique to the magnetic field:

$$\sphericalangle (\mathbf{v}, \mathbf{B}_0) \equiv \theta > (m/M)^{1/2};$$

$$\delta \sim (c/\omega_p)(M/m)^{1/2}\theta.$$

The corresponding shock structure is sketched in Fig. 8.

More complicated dispersion laws can produce solitons of quite exotic shape. For example, if we have two ion species and thus two branches to the dispersion relation (propagation $\perp B$; see Fig. 9), the wave train of solitons appears as in Fig. 10.

For many uses where the quadratic approximation to the dispersive correction is adequate, the Korteweg–de-Vries equation is often used as a quite general, reasonably simple model which describes the competition between nonlinearity and dispersion:

$$\frac{\partial V}{\partial t} + V \frac{\partial V}{\partial x} = \alpha \frac{\partial^3 V}{\partial x^3}.$$

The analysis of this equation led to an exciting break-

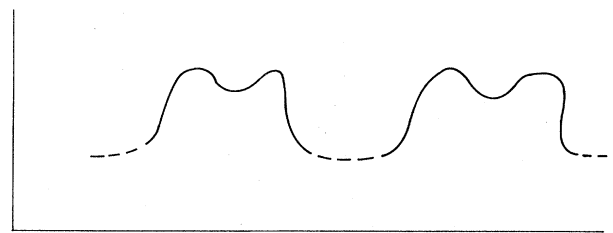FIG. 8. The oscillatory shock profile in the case of rarefaction solitons.

FIG. 10. The oscillatory shock which results from the dispersion law of Fig. 9.

through in nonlinear mathematical physics. Kruskal and his collaborators showed in 1967 that inverse scattering techniques, originally developed in quantum mechanics, could be used to generate exact solutions of the Korteweg–deVries equation. Subsequently, many other related nonlinear equations were also attacked successfully using the inverse scattering technique. Nevertheless, most of the remaining problems in collisionless shock theory lie, for physical reasons, completely outside the scope of the Korteweg-deVries equation or, more generally, the inverse scattering technique. Let us first list, then discuss, three of the most important outstanding problems:

(1) particle orbits and effects of thermal motion;
(2) $\mathfrak{M} > \mathfrak{M}_c$;
(3) instabilities and turbulence.

1. Particle orbits

The interaction of particle thermal motion with the oscillatory structure leads to dissipation of the wave energy. In magnetic shocks, the magnetic moment need not be conserved (Fig. 11). Furthermore, we can have particle reflection (Fig. 11). The reflected ions would stream ahead of the shock carrying the perturbations of density and field at a speed greater than the shock speed. This means that the total profile is no longer in steady state; the "foot" or "pedestal" (immediate preshock portion of the waveform) will run away. This process could be stopped only by transverse or nearly transverse magnetic fields $(u \perp B)$; in this case, the size of the pedestal would be of the order of a gyroradius. Instabilities produced by the reflected beam would also eventually stop the pedestal runaway. Magnetic modes seem most efficient for this purpose. Some of these effects have already been studied numerically (Biskamp, 1973).

2. $\mathfrak{M} > \mathfrak{M}_c$

For sufficiently large-amplitude perturbations, steady-state wave solutions no longer exist—the dispersion, at last, cannot compete with the nonlinear steepening. The same thing happens to shallow water solitary waves, as we well know. This wavebreaking signifies the breakdown of the moment approximation; the plasma no longer behaves like a fluid, the motion becomes multistreaming and likely unstable. The latter means that an effective "turbulent viscosity" would
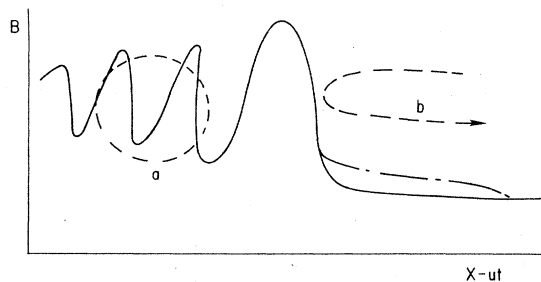

FIG. 11. Some realistic phenomena in shocks. (a) Magnetic moment is not conserved in regions of steep gradients (magnetic shocks only). (b) Particle reflection. (———) Shock profile in absence of reflection. (— — —) Profile with reflection; the "pedestal."

be important.

In some sense, the wavebreaking and multistreaming is a limiting case of a very pronounced pedestal. If this runaway multistreaming is stopped by a transverse magnetic field, the thickness of the resulting shock becomes of the order of several gyroradii. This kind of shock has again a close analog in shallow water hydrodynamics—the so-called hydrodynamic bore.

Before the multistreaming could be mixed due to the Larmor rotation, it might well be unstable. The lower hybrid mode is probably the fastest growing, with $\text{Im}\,\omega \sim (\omega_{ce}\omega_{ci})^{1/2}$. For oblique shocks, whistler generation may predominate. A potential mixer for the multistreaming would be the ion-ion beam acoustic instability. However, it is believed that this saturates at a too low level of turbulence, producing only a minor change in the multistreaming ion distribution function. Thus, if the plasma supports only ion acoustic modes, it is likely that there will be no collisionless shocks for sufficiently high Mach numbers, $\mathfrak{M} \gtrsim 3–5$.

3. Instabilities and turbulence

There are various instabilities which transform the energy of regular (laminar) nonlinear motion (wave trains) first into chaotic, turbulent motion, then into random particle motion. The most obvious mechanism is the parametric decay instability of the almost periodic wave trains of the oscillatory shocks: $\omega_0 \rightarrow \omega_1 + \omega_2$, $k_0 \rightarrow k_1 + k_2$. As a consequence, the regular nonlinear oscillations would be damped more rapidly than the theory of laminar shocks would predict, since the energy is transferred to the entire noise spectrum. This decay type of instability would be more appropriate for dispersion with $\Delta(\omega/k) > 0$.

For nonlinear waves in a magnetic field, the most obvious type of instability is the beam instability, when the mean electron velocity relative to the ions exceeds the mean electron thermal velocity $[v_y > (T_e/m_e)^{1/2}]$. Physically, this instability says that the electrons moving relative to the ions lose momentum and energy not only because of ordinary collisions, but also because of anomalous electric resistivity. We expect, of course, that the bulk of the energy will go into the electrons (see Lecture I). Thus the effective electron temperature will increase relative to that of the ions. At some point, then, ion acoustic instability must become operative. For this case, we already know the anomalous resistivity $\sigma = ne^2/m\nu^*$ (see Lecture I). It is then a standard procedure to find the shock thickness; in analogy to the viscous dissipation discussed earlier, one finds that the anomalous resistivity leads to a shock thickness

$$\Delta_{sh} \sim c^2/(4\pi u\sigma^*).$$

When we consider the possibility that the plasma exhibits nonfluid-like behavior (that is, when a particle kinetic equation must be used), the collisionless shock situation becomes extremely complicated. When one allows only free-streaming ($B_0 = 0$), no simple models of collisionless shocks exist. Note that we have already discussed a similar situation; multistreaming at $\mathfrak{M} > \mathfrak{M}_c$ remain valid here. Therefore it is quite probable that when one does not permit magnetic modes, there will
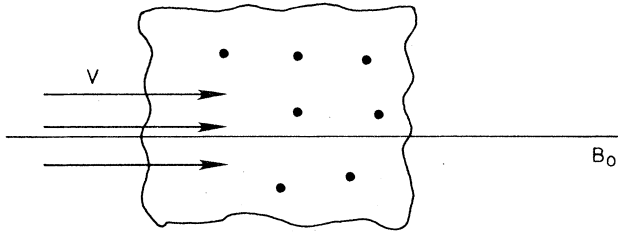
FIG. 12. Plasma streaming along an unperturbed magnetic field B_0. A small volume element is shown.

be no collisionless, turbulent shocks. Numerical simulations are of great help in this complicated business. Much more computational effort is required.

Various mechanisms can prevent particle free-streaming. We will now discuss one of the best understood, the so-called "fire hose" instability. Let us consider free-streaming parallel to the direction of the unperturbed magnetic field. What is the subsequent plasma behavior in the presence of a small perturbation? The net particle distribution in a small volume element consists of the superposition of the unperturbed plasma and the perturbed particles which stream into the volume element (Fig. 12). This distribution is obviously anisotropic, with the parallel pressure

$$P_\parallel = m \int d\mathbf{v}(v_\parallel - \bar{v}_\parallel)^2 f(\mathbf{v})$$

growing faster than the perpendicular pressure $P_\perp$. As a function of time, the pressure $\Delta p \equiv p_\parallel - p_\perp$ within the given volume element would behave qualitatively like curve (a) in Fig. (13). We expect an instability when $\Delta p > B_0^2/4\pi$. When the instability threshold is exceeded, a drastic change in the free-streaming will result. Let us discuss briefly the physics of this change. The perturbation will lead to fluctuations in the magnetic field lines. The particle flow along the curved field lines gives rise to a centrifugal force, for each particle $F_c \sim m v_\parallel^2/R$ or summed over all particles $F \sim p_\parallel/R$. (R is the effective radius of curvature of the line.) This force in turn tends to increase the curvature, maintaining the instability (Fig. 14). Thus the mechanism makes the magnetic lines turbulent. As the turbulence level $\langle \delta B^2/8\pi \rangle$ grows, it will react back on the particle distribution via the quasilinear effect. This we can estimate qualitatively. Since the instability is low frequen-
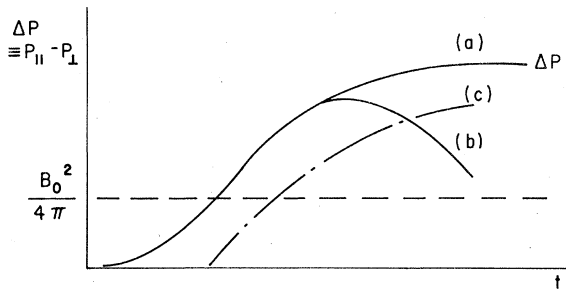

FIG. 13. Time dependence of anisotropy ΔP due to free-streaming $\parallel B$. (a) ΔP in absence of quasilinear modification of particle distribution. (b) ΔP with quasilinear effect. (c) Associated growth of magnetic fluctuations $W = \langle \delta B^2 \rangle/8\pi$.
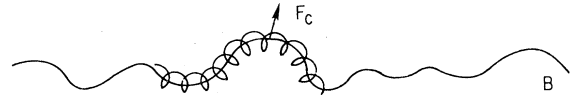

FIG. 14. Centrifugal distortion of field lines in firehose instability.

cy, the parallel adiabatic invariant $J = \int dl v_\parallel$ should be conserved for each particle. (dl is the arc length along a magnetic field line.) Since the effective line length grows as the turbulence develops, we would predict $dp_\parallel/dt < 0$, while $dp_\perp/dt > 0$ from the conservation of magnetic moment. Curve (b) on Fig. 13 shows the expected behavior of Δp, while curve (c) shows the associated growth of magnetic energy in the fluctuations. The situation is reminiscent of the isotropizing effect of collisions in an ordinary gas; in the present case, the "collisions" are scattering on the magnetic field irregularities, which are themselves produced by the plasma in a nonlinear, self-consistent way. The particle motion also reminds us of the problem of cosmic ray diffusion in random magnetic fields.

In the "fire hose" problem, the difficulty, of course, lies in the self-consistent description of the turbulence. However, if $\Delta p \gg B_0^2/4\pi$, we can use weak turbulence theory. In particular, we can use quasilinear equations to describe the kinetic interactions of the particles with the turbulent fields. In the present case, the equation for the space-averaged distribution $\langle f \rangle$ is of the form (Sagdeev and Galeev, 1969)

$$\frac{d\langle f \rangle}{dt} = \frac{e^2}{2m^2c^2\omega_0^2} \left[v_\perp^2 \frac{\partial^2\langle f \rangle}{\partial v_\parallel^2} + v_\parallel^2 \frac{1}{v_\perp} \frac{\partial}{\partial v_\perp} v_\perp \frac{\partial\langle f \rangle}{\partial v_\perp} \right. $$
$$\left. - 2v_\perp \frac{\partial}{\partial v_\parallel} v_\parallel \frac{\partial\langle f \rangle}{\partial v_\perp} \right] \frac{dW}{dt}, \qquad (3)$$

where W is the energy density in the magnetic fluctuations in dimensionless units:

$$W \equiv \sum_k |\delta B_k|^2 / |B_0|^2.$$

The spectrum evolves according to

$$\frac{d}{dt} |\delta B_k|^2 = 2\gamma_k |\delta B_k|^2, \qquad (4a)$$

where

$$\gamma_k = \frac{k}{(Mn)^{1/2}} \left(p_\parallel - p_\perp - \frac{B_0^2}{4\pi} \right)^{1/2}. \qquad (4b)$$

Let us consider a steady-state situation in which all quantities vary as $x-ut$. If we use the magnetic energy W instead of the time as an independent variable, Eq. (3) becomes in the moving frame

$$(v_\parallel - u_0)\frac{\partial\langle f \rangle}{\partial W} = -u_0 v_\perp^2 \frac{\partial^2\langle f \rangle}{\partial v_\parallel^2} + \cdots. \qquad (5)$$

Solution of this equation is not completely straightforward because of its singular character; however, this solution has been carried through (Galeev and Sagdeev, 1969). We will not repeat those details here; however, we can show that shock-like solutions arise by using simplified estimates. Two different contributions to the pressure anisotropy are: adiabatic relaxation and quasi-
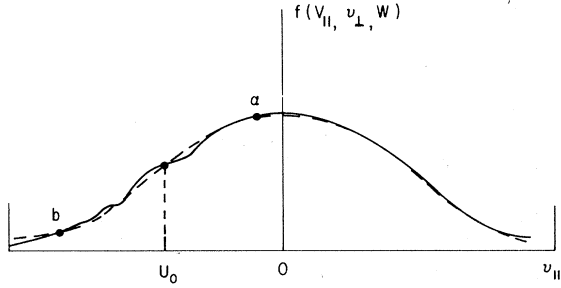
FIG. 15. Quasilinear modification of the ion distribution function: (-----) Maxwellian distribution ahead of the shock front. (——) ion distribution after quasilinear relaxation. (a) and (b) show the comparison between the quasilinear slope and the slope of Maxwellian distribution for different positions of the resonant velocity.

linear relaxation of the distribution function in the vicinity of the singular point $v_{\parallel} = u_0$. Adiabatic relaxation is described by Eq. (3). Taking the appropriate moments, we find that this contribution to the pressure anisotropy is proportional to wave energy and negative (stabilizing):

$$p_{\parallel} - p_{\perp} \approx - \text{const } W \text{ (negative)} .$$

(Here and later we neglect the small magnetic tension for $B_0^2/4\pi \ll p_0$.) Quasilinear relaxation in the vicinity of the resonant velocity $v_{\parallel} = u_0$ is described by Eq. (5). We see that a simple quasilinear "plateau" $(\partial f/\partial v_{\parallel} = 0)$ does not represent the solution of this equation, so the distribution function has some finite slope as a result of relaxation. For small resonant velocity u_0, this slope is larger than for Maxwellian distribution (case a of Fig. 15); as a result, the pressure anisotropy decreases with W. That means stabilization of the fire hose instability. But for sufficiently large velocity u_0, quasilinear effects become destabilizing (case b of Fig. 15). The increase in pressure anisotropy with the wave energy growth for the latter case could be estimated as follows:

$$\Delta(p_{\parallel} - p_{\perp}) = \int m\left(v_{\parallel}^2 - \frac{v_{\perp}^2}{2}\right)(f_{QL}(v_{\parallel}, v_{\perp}, W) - f_M(v_{\parallel}, v_{\perp})) .$$

Taking into account that the main contribution to the integral comes from the vicinity of the resonant velocity $v_{\parallel} = u_0$ with the width $\Delta v_{\parallel} \sim (u_0 v_{\perp}^2 W)^{1/3}$ [see Eq. (5)], we obtain in order of magnitude

$$\Delta(p_{\parallel} - p_{\perp}) \sim m \int_{u_0 - \Delta v_{\parallel}}^{u_0 + \Delta v_{\parallel}} u_0(v_{\parallel} - u_0)$$

$$\times \left(\frac{\partial f_{QL}}{\partial v_{\parallel}} - \frac{\partial f_M}{\partial v_{\parallel}}\right)\Big|_{v_{\parallel} = u_0}(v_{\parallel} - u_0)dv_{\parallel}$$

$$\sim m n_0(\mathfrak{M}^2 - 1)(\Delta v_{\parallel})^2 \sim (\mathfrak{M}^2 - 1)p_0 W^{2/3} \text{ (positive)} .$$

(6)

Here the factor $(\mathfrak{M}^2 - 1)$ is responsible for the change of the relative slope of the quasilinear and Maxwellian distribution functions at some critical resonant velocity $u_{0,cr}$ $(\mathfrak{M}^2 = u_0^2/u_{0,cr}^2)$. Combining the adiabatic and resonant contributions to the pressure anisotropy, we obtain

$$p_{\parallel} - p_{\perp} = (\mathfrak{M}^2 - 1)p_0 W^{2/3} - \text{const } W .$$

With the help of this equation, it is then easy to see the existence of a shock-like solution (see Figs. 13 and 16),

FIG. 16. The shock-time solution admitted by the quasilinear equations of the fire hose instability.

with a characteristic spatial scale length of the order of a few ion gyroradii. Strictly speaking, this solution is restricted to weak turbulence, $\mathfrak{M} - 1 < 1$. However, the "fire hose" mode is a viable scattering mechanism for all Mach numbers—in fact, it should be even more effective at high $\mathfrak{M}$, since $p_{\parallel} \sim \mathfrak{M}^2 c_s^2$.

For the "fire hose" mode, it was essential to have a small but finite B_0. What about the limiting case $B_0 \equiv 0$? Here, too, there is a magnetic mode due to the anisotropy of the particle distribution—the so-called Weibel mode. Let us again consider the situation of Fig. 12, but with $B_0 \equiv 0$. If we associate the parallel index "$\parallel$" with the free-streaming direction y, then once again $p_{\parallel}$ will become larger after interpenetration than $p_{\perp}$. This means, for example, that the effective temperature T_y will be larger than T_z. Let us consider the linear stability of such a plasma against magnetic perturbations $\delta B = \hat{x}\delta B_x \exp[i(kz - \omega t)]$. If we think about particle orbits in the vicinity of $\delta B = 0$, then it is easy to see (Fig. 17) that the motion will be such as to produce a current in the y direction with a sign such that the induced magnetic field enhances the original magnetic perturbation. This produces a pinching of the current perturbations, and an instability. It should also be clear from this argument that thermal motion in the z direction would tend to stabilize this instability.

Mathematically, the linear behavior of this instability follows from the linearized Vlasov–Maxwell equations. With $\delta B = \nabla \times \delta A = -ik\delta A_y \hat{x}$, and neglecting displacement current, these read

$$-i(\omega - kv_z)\delta f + i\frac{e}{mc}\delta A_y\left[(\omega - kv_z)\frac{\partial f_0}{\partial v_y} + kv_y\frac{\partial f_0}{\partial v_z}\right] = 0 ;$$

$$k^2\delta A_y = \frac{4\pi}{c}\delta j_y ;$$

$$\delta j_y = \sum_s (ne)_s \int dv v_y \delta f .$$

Combining these gives readily the dispersion relation

$$k^2 = \sum_s \frac{\omega_p^2}{c^2}\left[\int d\mathbf{v}\frac{kv_y^2}{\omega - kv_z}\frac{\partial f_0}{\partial v_z} - 1\right] .$$

In the limit where $\omega/k \ll v_{t_i}$, this simplifies to
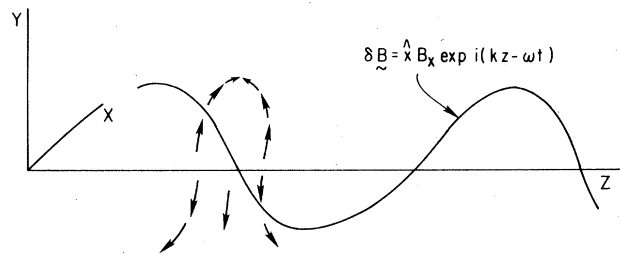

FIG. 17. Physical mechanism for current pinching and the Weibel instability. The arrows indicate particle orbits in a vicinity where $\delta B = 0$.
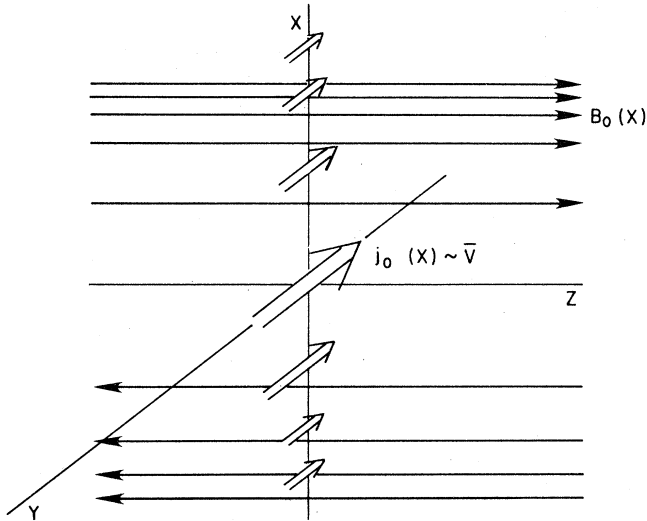
FIG. 18. Simple equilibrium with neutral layer.

$$k^2 \simeq -\left(\frac{\Delta T}{T}\right)\left(\frac{\omega_{pe}^2}{c^2}\right) - \frac{\omega^2}{c^2}\frac{1}{(k\lambda_D)^2} + v\frac{\pi}{2}i\frac{\omega_{pe}^2}{c^2}\left(\frac{\omega}{kv_{te}}\right), \tag{7}$$

where

$$\Delta T \equiv T_z - T_y .$$

We have assumed $|\Delta T| \ll 1$ and also dropped terms small in the square root of the mass ratio. We see that instability is possible for $\Delta T < 0$. More specifically, the growth rate is positive for

$$k^2 < -\frac{\omega_{pe}^2}{c^2}\left(\frac{\Delta T}{T}\right).$$

In this limit, one can show that the wave is a negative energy mode.

As the instability develops, we expect the current pinches to develop randomly throughout the plasma. There is as yet no successful nonlinear theory for the self-consistent, effective scattering of these random pinches. Thus it remains an interesting open question to find the shock thickness.

III. NEUTRAL LAYERS

We can now make a smooth transition to the problem of neutral layers, collisionless tearing modes, and the reconnection of magnetic field lines. Such a situation occurs in the earth's magnetic tail. Quite remarkably, in fact, the same mode we just discussed in collisionless shock theory is also crucial for tearing in neutral layers. Physically, this is because the relative drift of electrons through ions is in a sense equivalent to anisotropy. We may thus expect an effective $\Delta T \sim \bar{v}^2$. In general, the linear theory is more complicated here, since in the neutral layer problem we have a nonuniform equilibrium (Fig. 18). However, we can simplify the problem by noting that the particles are effectively unmagnetized within a region around $B_0 = 0$ of thickness $d_{e,i} \sim (a_{e,i}L)^{1/2}$, where $a_{e,i}$ is the electron or ion gyroradius, and L is the thickness of the neutral layer. Only the unmagnetized particles will contribute to the Landau resonance term $i\pi (\omega_p^2/c^2)(\omega/k v_{te})$. The problem can now be cast
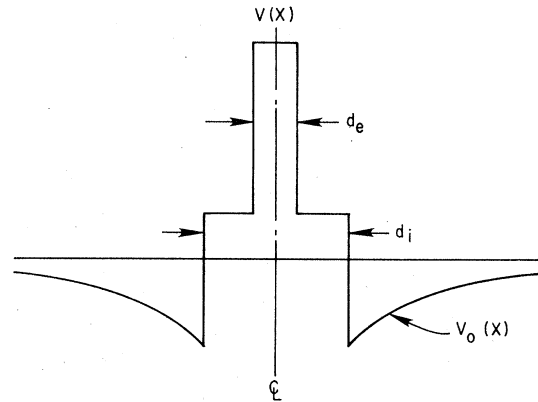

FIG. 19. The model potential for the 1–D Schrödinger equation for the tearing eigenmode.

as an eigenvalue problem, equivalent to a Schrödinger equation with the effective potential sketched in Fig. 19. In fact, if we are clever, we can find the equation for the tearing eigenmode by analogy with Eq. (7) for the Weibel mode. In the present case, we have a nonuniform equilibrium $B_0(x)$, so we should replace k_z^2 by k_1^2:

$$k_z^2 \to k_z^2 - \frac{d^2}{dx^2}.$$

The equation for the y component of the vector potential then becomes

$$\frac{d^2A}{dx^2} - \left\{ k_z^2 + v_0(x) + \left[\frac{\omega^2}{c^2}\frac{1}{(k_z\lambda_D)^2} \right. \right.$$
$$\left. \left. -i\left(\frac{\pi}{2}\right)^{1/2}\frac{\omega_p^2}{c^2}\frac{\omega}{k_z v_{te}} \right] \right\} A = 0, \tag{8}$$

where the terms in square brackets are to be taken only in the inner region $x < (a_e L)^{1/2}$, and where $v_0(x)$ plays the role of the effective ΔT. For calculating v_0, it is computationally convenient to take as zero-order distribution the Harris equilibrium, constructed from the constants of the motion v^2 and $p_y = mv_y + eA_y/c$. We choose a form

$$f_j \sim \exp\left(-\frac{mv^2}{2T_j} + \bar{v}_j\frac{p_y}{T_j}\right),$$

where $\bar{v}_0 T = $ const. This we rewrite in the more convenient form of a Maxwellian distribution

$$f_j(\mathbf{v}) = n(x)\left(\frac{m_j}{2\pi T_j}\right)^{3/2}\exp\left\{\frac{-1/2\, m_j[v_x^2 + (v_y - \bar{v}_j)^2 + v_z^2]}{T_j}\right\},$$

where

$$n(x) = n_0\exp\left[\frac{e_j\bar{v}_j}{cT_j}A_y(x)\right],$$

and $\bar{v}_j \sim T_j/e_j$. Using Ampere's law

$$A'' = 4\pi/c\sum_j n_j(x)e_j\bar{v}_j,$$

with boundary conditions

$$dA_j/dx(0) = 0\,; \; A_y = \pm B_0 x, x \to \pm\infty,$$

we obtain the equation for magnetic field profile

$$\left[\frac{dA}{d(x/L)}\right]^2 = 1 - \exp\left[\alpha A\left(\frac{x}{L}\right)\right],$$

where

$$A\left(\frac{x}{L}\right) = \frac{A_y(x)}{B_0 L}, \alpha \equiv \frac{e_j B_0 L}{cT_j} \quad \bar{v}_j; \frac{B_0^2}{8\pi} = n_0(T_i + T_e).$$

For $\alpha = -2$, this equation gives a very simple solution:

$$B_z(x) = B_0 \tanh(x/L).$$

The corresponding density profile (to satisfy pressure balance) is

$$n(x) = n_0 \cosh^{-2}(x/L).$$

The presence of current velocity $\bar{v}_j = -2cT_j/e_j B_0 L$ is equivalent to the increase of pressure in the y direction

$$\frac{\Delta p_y}{p_{th,y}} = \frac{m_j \bar{v}_j^2}{T_j}.$$

Substituting this expression into dispersion relation (7) and using pressure balance, we obtain the function $v_0(x)$

$$v_0(x) = -\sum_j \frac{\omega_{pj}^2(x)}{c^2} \frac{m_j \bar{v}_j^2}{T_j} \equiv -\frac{2}{L^2} \frac{1}{\cosh^2(x/L)}.$$

Using this form of v_0 in Eq. (8) for the external region, we see that a solution for $\omega = 0$, the instability boundary, is $A = [\cosh(x/L)]^{-1}$ with the eigenvalue condition yielding $kL = 1$ as the criterion for marginal stability. For $kL < 1$, the system is unstable. To find the growth rate, for small $(1 - k^2 L^2)$, we can use a familiar perturbation technique from one-dimensional quantum mechanics (the "shallow potential well approximation")

$$\frac{1 - k^2 L^2}{L^2} \int_{-\infty}^{+\infty} \frac{dx}{\cosh^2(x/L)}$$

$$= -i\left(\frac{\pi}{2}\right)^{1/2} \int_{-d_e}^{+d_e} \frac{\omega_p^2}{c^2}\left(\frac{\omega}{k_z v_{te}}\right) \frac{dx}{ch^2(x/L)}.$$

$$(9)$$

Then we find

$$\gamma = \frac{2\sqrt{2}}{\pi^{1/2}} \frac{v_{te}}{L}\left(\frac{a_e}{L}\right)^{3/2}(1 - k^2 L^2).$$

In applying this technique to the magnetic field reconnection in the geomagnetic tail, it is very important to discuss plasma configurations with small normal components of equilibrium magnetic field (see Fig. 20a): $B = B_0 \tanh(x/L)\hat{y} + B_\perp \hat{x}$. Though more difficult than before, this case can also be treated rather exactly (Galeev and Zelenii, 1975). We give here only a qualitative discussion. The Larmor rotation of the particles in the normal magnetic field gives an additional mechanism for breaking of the usual resonant interaction between the particles and the perturbation. The condition that the resonance be unimportant is simply that $\omega_{cl} > \gamma$, where γ is the growth rate and ω_{cl} is the gyrofrequency in the normal magnetic field. As we raise $B_\perp$ from zero, this is satisfied first for electrons, at roughly

$$b \equiv B_\perp/B_0 \sim (a_e/L)^{5/2} \equiv b_{ie}.$$

At this point, the resonant contribution $-i\pi(\omega_p^2/c^2)(\omega/k_z v_t)$ goes over to $(\omega_p^2/c^2)(\omega_{cl}/k_z v_t)$. This term is positive, of sign opposite to $v_0(x)$; it is therefore stabiliz-
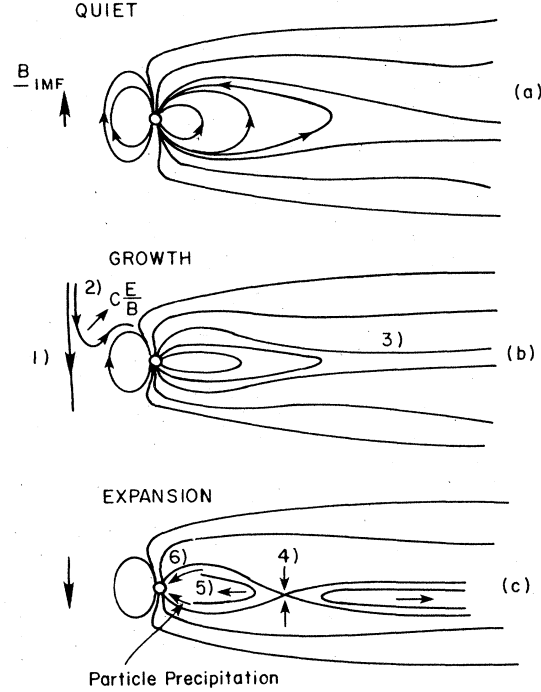
FIG. 20. Qualitative scenario for magnetospheric substorms.

ing. More generally, let us denote this contribution by δv. As we continue to increase b, δv will grow $\sim \omega_{cl}$. One can show that it reaches a maximum at $k_z^2 a_{el}^2 \sim 1$, after which it decreases with $B_\perp$ roughly as $B_\perp^{-2}$. Eventually, the contribution of the δv term to the dispersion relation (9) becomes less than that of $v_0(x)$ and we will once more have the tearing instability, this time, however, due to the ion resonance. With still larger $B_\perp$, the ion trajectories are also modified and δv again becomes stabilizing. Referring to Fig. 21, the mode will be unstable in the gap $b'_{2e} < b < b_{1i}$, as well as $b < b_{ie}$.

Considerations along this line lead to the stability diagram shown in Fig. 22. By a metastable region, we mean parameters for which the system is stable against small perturbations, but may be moved into the unstable regime by a fluctuation of sufficiently large amplitude. Also shown in Fig. 20 is a possible sequence of events proposed by Galeev and Zelenii (1976) to explain the phenomena associated with magnetic substorms. We will just sketch this scenario, without citing supporting experimental evidence or even giving all the logical steps in the argument. We refer to Figs. 20 and 22. Briefly, the appearance of a neutral point at the nose of the magnetosphere (1) is followed by an $E \times B$ drift of the magnetic field lines to the tail (2). The tail then narrows, corresponding to a decrease of the normal component b and an increase in the inhomogeneity ε(3). This brings the tail into the metastable regime; it is followed by the onset of the (ion) tearing instability and the formation of a reconnection point (4). This in turn leads to intense particle flows and precipitation (5, 6).

It is fitting to close these lectures by commenting on the similarities and differences between the collisionless tearing mode we have been discussing in the context of space and astrophysical applications, and the resistive
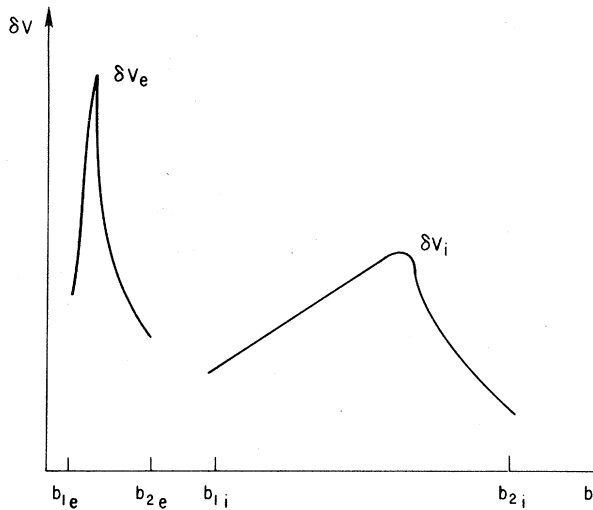
FIG. 21. Resonant contribution δV to real part of effective potential V, for tearing layer with normal magnetic field ($b \equiv B_\perp/B_0$).

tearing mode thought to play a major role in the MHD behavior of Tokamaks, of considerable interest in the quest for thermonuclear fusion. The equations are more complicated in the collisionless case (since we must deal with complicated particle orbits), while the geometry is more complicated in the MHD case. For the resistive mode the linear theory has long been known (Furth *et al.*, 1963), while the most general linear stability analysis for the collisionless case consists as yet of only speculations. By contrast, the nonlinear theory has been carried much farther in the MHD case, where 2-*D* models have been developed and extensively studied (White *et al.*, 1976). For the 3-*D* resistive case, we
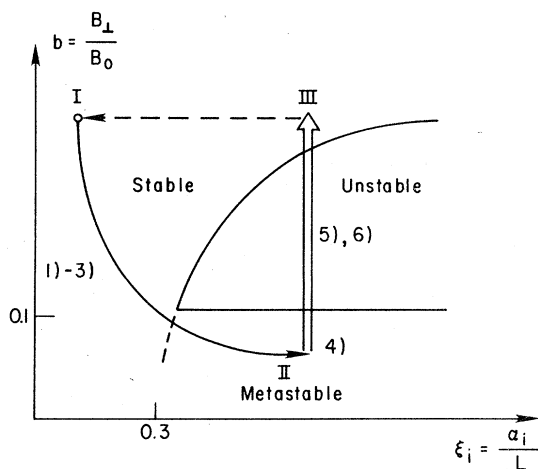

FIG. 22. Stability regimes for the collisionless tearing mode. The cycle of events I–II–III is Galeev's and Zelenii's scenario for the interpretation of magnetic substorms. The numbers (1)–(6) are keyed to Fig. 20.

have as yet only the qualitative scenario by Kadomtsev (1976). There is some hope that certain of these nonlinear considerations bear on the collisionless case as well.

In conclusion, the phenomena of shocks and discontinuities have significant places in many problems of current interest, both in astrophysical applications and in the laboratory. Our understanding of these matters has improved considerably over the last decade; however, there is yet much to be learned. Particularly noteworthy is the close connection of the shock-like phenomena discussed in the present lecture to the phenomena of plasma turbulence discussed in Lecture I. We cannot truly understand the former until we have mastered the latter. The proper marriage of these two aspects of plasma physics represents a major goal for the future.

In these two lectures, I have tried to point out some of the most interesting and important problems of nonlinear plasma physics. In these few short hours, I have really only scratched the surface. It should be clear, though, that plasma physics is a vital and alive science, rich with fascinating problems and important applications. The challenge of gaining a yet better understanding of the nonlinear plasma medium is one hard to ignore.

REFERENCES

Biskamp, D., 1973, "Collisionless Shock Waves in Plasmas," Nucl. Fusion **13**, 719.

Furth, H. P., J. Killeen, and M. N. Rosenbluth, 1963, "Finite-Resistivity Instabilities of a Sheet Pinch," Phys. Fluids **6**, 459.

Galeev, A. A., 1976, "Collisionless Shocks," in *Physics of the Solar-Terrestrial Environment,* edited by D. Williams (American Geophysical Union, Washington D. C.).

Galeev, A. A., and R. Z. Sagdeev, 1969, "Model of a Shock Wave in Solar Wind Plasma," Zh. Eksp. Teor. Fiz. **57**, 1047 [Sov. Phys.-JETP **30**, 571 (1970)].

Galeev, A. A., and L. M. Zelenii, 1975, "Nonlinear Instability Theory for a Diffusive Neutral Layer," Zh. Eksp. Teor. Fiz. **69**, 882 [Sov. Phys.-JETP **42**, 450 (1976)].

Galeev, A. A., and L. M. Zelenii, 1976, "Role of Plasma Processes in Substorm Dynamics," Paper TS-3-39, *Physics of the Solar-Terrestrial Environment,* edited by D. Williams (American Geophysical Union, Washington D. C.).

Kadomtsev, B. B., 1977, "Reclosing of Lines of Force and Disruptive Instabilities in Tokamaks," in *Proceedings of the 6th International Conference on Plasma Physics and Controlled Nuclear Fusion Research* (IAEA, Vienna), Paper B1.

Sagdeev, R. Z., 1966, "Cooperative Phenomena and Shock Waves in Collisionless Plasmas," in *Reviews of Plasma Physics,* edited by M. A. Leontovich (Consultants Bureau, New York), Vol. 4, p. 23.

Sagdeev, R. Z., and A. A. Galeev, 1969, *Nonlinear Plasma Theory,* edited by T. M. O'Neil and D. L. Book (Benjamin, New York).

White, R. B., D. A. Monticello, M. N. Rosenbluth, and B. V. Waddell, 1977, "Nonlinear Tearing Modes in Tokamaks," in *Proceedings of the 6th International Conference on Plasma Physics and Controlled Nuclear Fusion Research* (IAEA, Vienna), Paper B2-1.